Supplementary Information

Dynamics of fluorinated imide-based ionic liquids using Nuclear Magnetic Resonance techniques

Tawhid Pranto[a,b], Carla C. Fraenza[c,*1], Frederik Philippi[d], Daniel Rauber[e], Christopher W. M. Kay[e,f], Tom Welton[d], Steven G. Greenbaum[a,c], Sophia Suarez[a,b,*]

[a]Department of Physics, The Graduate Center of CUNY, New York, NY, USA.

[b]Department of Physics, Brooklyn College of CUNY, New York, NY, USA.

[c]Department of Physics & Astronomy, Hunter College of CUNY, New York, NY, USA.

[d]Department of Chemistry, Molecular Sciences Research Hub, Imperial College London, London, UK.

[e]Department of Chemistry, Saarland University, Saarbrücken, Germany.

[f]London Centre for Nanotechnology, University College London, London, UK.

*Corresponding authors

E-mail: carla.cecilia.fraenza@unc.edu.ar (Carla C. Fraenza),

snsuarez@brooklyn.cuny.edu (Sophia Suarez).

[1]Present address: IFEG-CONICET and National University of Cordoba, Cordoba, Argentina.

1. Self-diffusion coefficients measured by PFG-NMR

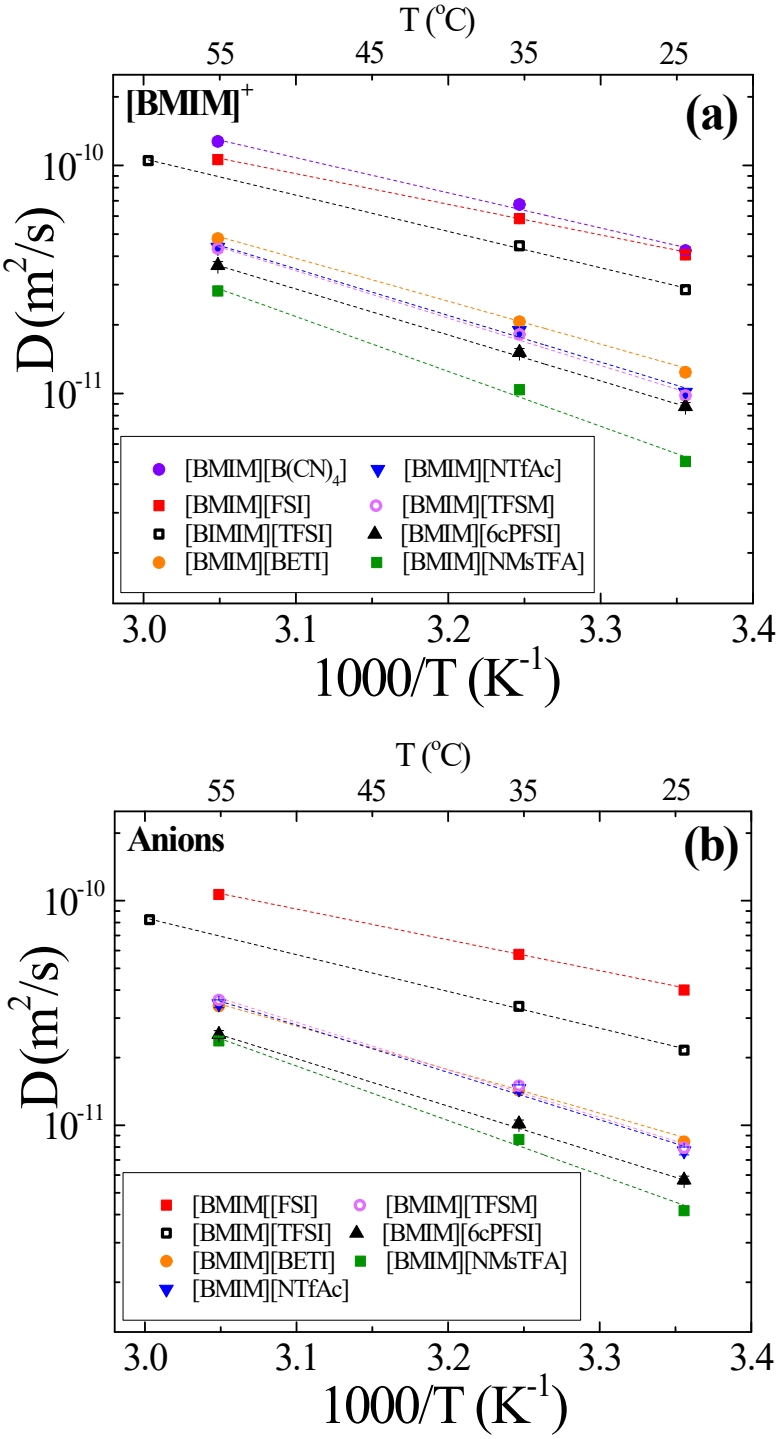

Figure S1. Temperature dependence of self-diffusion coefficients of **(a)** the $[BMIM]^+$ cation and **(b)** the anions ($[FSI]^-$, $[BETI]^-$, $[NTfAc]^-$, $[TFSM]^-$, $[6cPFSI]^-$ and $[NMsTFA]^-$) in the ILs. Self-diffusion coefficients for $[BMIM]^+$ and $[TFSI]^-$ in [BMIM][TFSI] are included for comparison purposes and the values at 60°C are taken with permission from reference (20). Lines represent the linear fittings of the data using an Arrhenius equation.

Table S1. Self-diffusion coefficients (D) for $[BMIM]^+$ (^1H) and the anions (^{19}F) in all studied ILs, at 25, 35 and 55°C.

Temperature (°C)	D [m²/s] × 10^{-12}														
	[BMIM][TFSM]		[BMIM][NMsTFA]		[BMIM][NTfAc]		[BMIM][6cPFSI]		[BMIM][BETI]		[BMIM][FSI]		[BMIM][B(CN)$_4$]	[BMIM][TFSI]	
	^1H	^{19}F	^1H	^{19}F	^1H	^{19}F	^1H	^{19}F	^1H	^{19}F	^1H	^{19}F	^1H	^1H	^{19}F
25	9.8 ±0.4	7.9 ±0.3	5.0 ±0.2	4.1 ±0.2	10.1± 0.4	7.7 ±0.3	8.8 ±0.3	5.7 ±0.2	12.4 ±0.5	8.5 ±0.2	40.5 ±1	40 ±2	42 ±1	28.5 ±1	21.6 ±0.9
35	18.0 ±0.7	15.0 ±0.6	10.4 ±0.4	8.6 ±0.3	18.9 ±0.7	14.5 ±0.6	15.2 ±0.6	10.1 ±0.4	20.6 ±0.8	14.3 ±0.6	58.5 ±2	57.7 ±2	67.4 ±2	44.4 ±2	33.8 ±1
55	43 ±1	36 ±1	28.1 ±1	23.7 ±0.9	43.8 ±1	34.8 ±1	36.4 ±1	25.4 ±1	47.8 ±2	34 ±1	106 ±4	106.5 ±4	128 ±5	------	------

2. Dispersions of the longitudinal relaxation rate

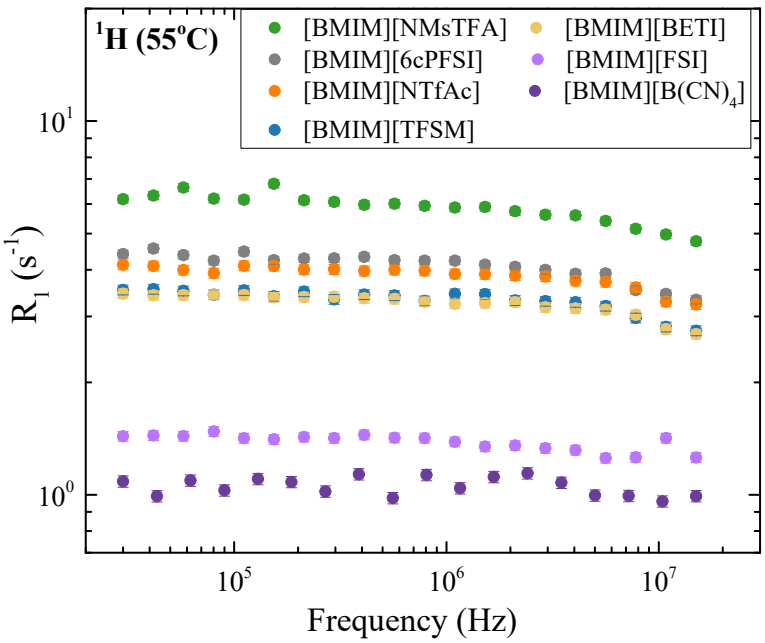

Figure S2. ^1H relaxation rate dispersions for [BMIM][NMsTFA], [BMIM][6cPFSI], [BMIM][NTfAc], [BMIM][TFSM], [BMIM][BETI], [BMIM][FSI], and [BMIM][B(CN)$_4$], recorded at 55°C. Frequencies are ^1H Larmor frequencies.

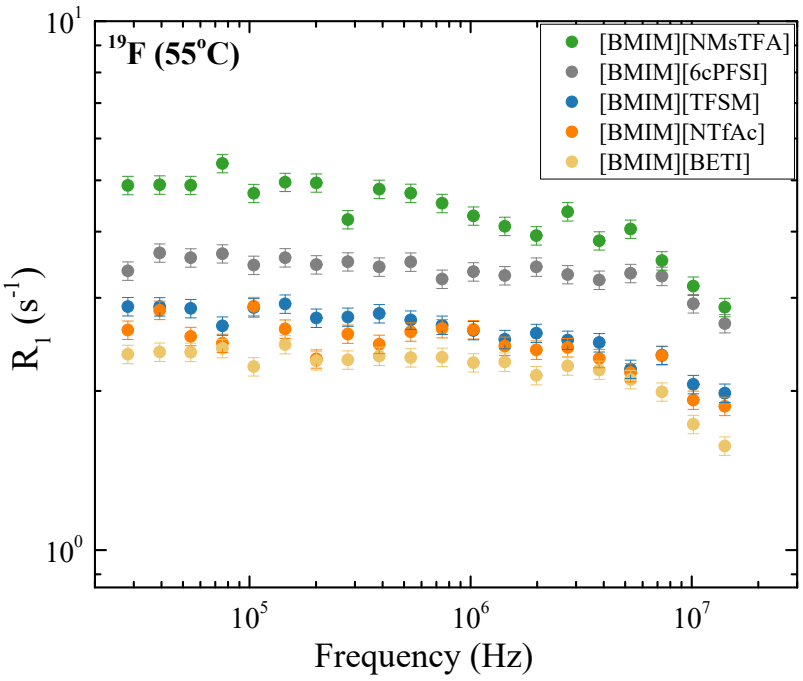

Figure S3. ^{19}F relaxation rate dispersions for [BMIM][NMsTFA], [BMIM][6cPFSI], [BMIM][TFSM], [BMIM][NTfAc], and [BMIM][BETI], recorded at 55°C. Due to the low signal-to-noise ratio, collecting anion dispersion data was impossible for [BMIM][FSI]. Frequencies are ^{19}F Larmor frequencies.

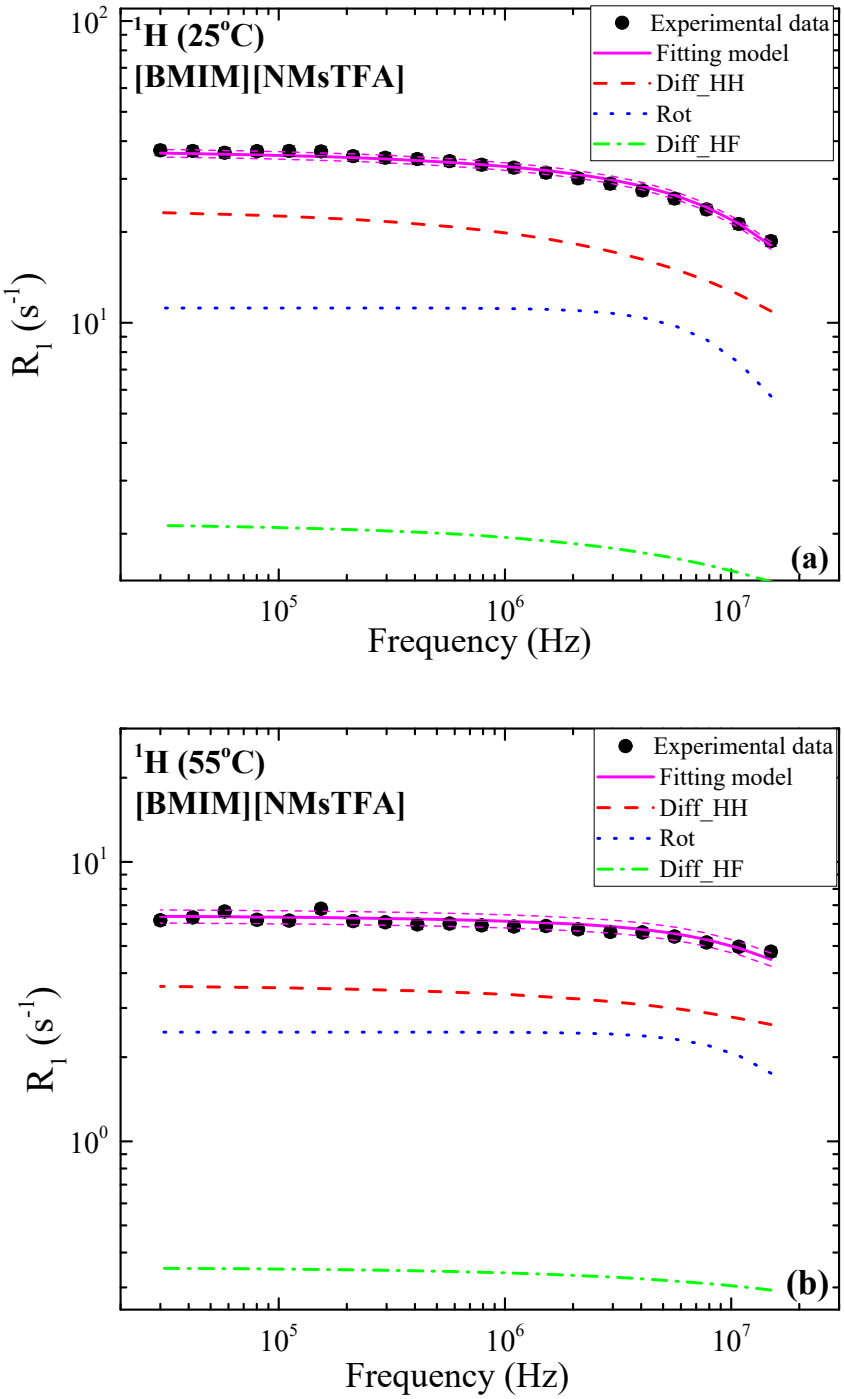

Figure S4. ^{1}H relaxation rate dispersions for [BMIM][NMsTFA] and their corresponding fittings using the model given by Eq. (7), recorded at 25°C **(a)** and 55°C **(b)**. Additionally, rotational contribution (Rot), and homonuclear (Diff_HH), and heteronuclear (Diff_HF) translational contributions are shown. Magenta dashed lines represent the fitting error. Frequencies are ^{1}H Larmor frequencies.

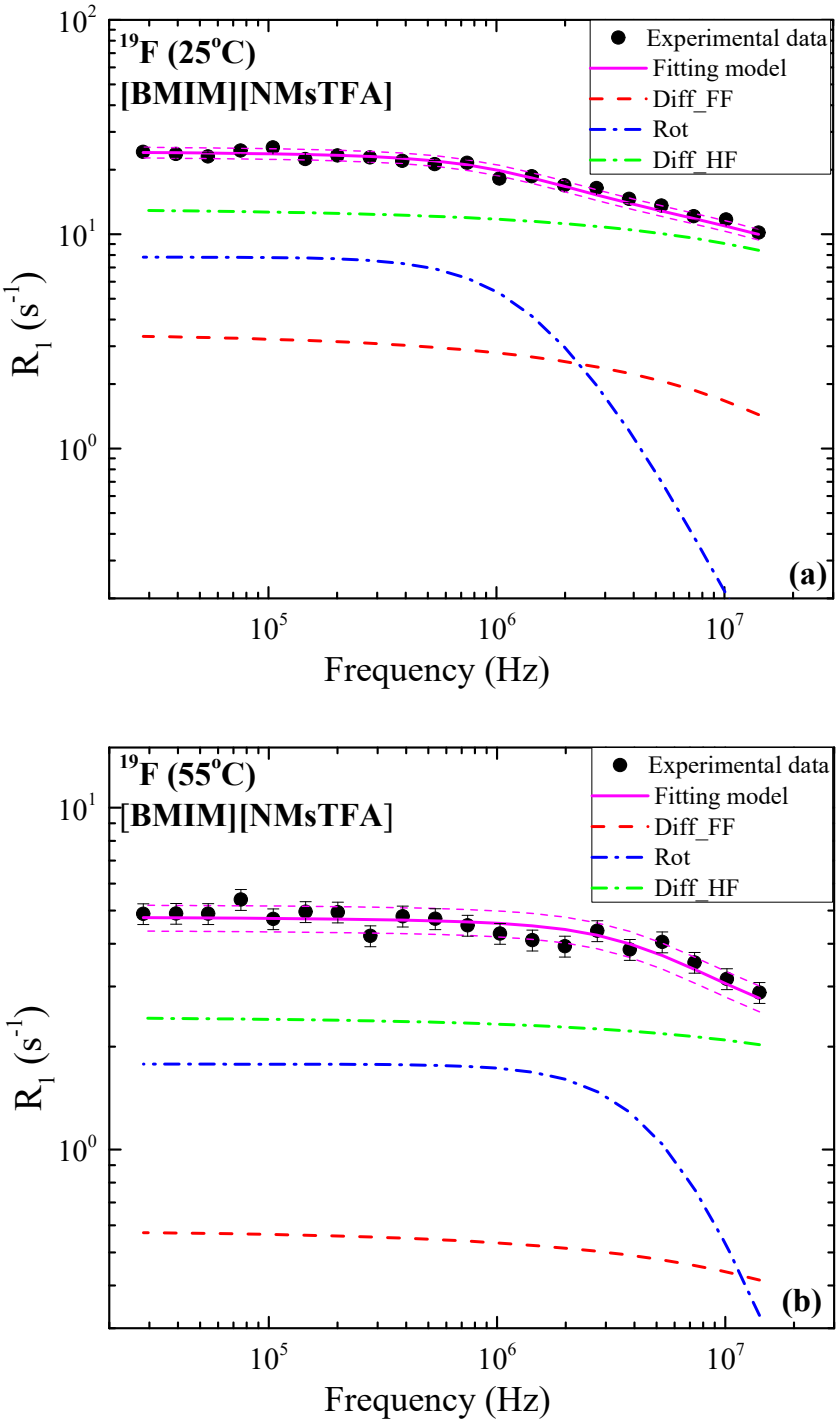

Figure S5. ^{19}F relaxation rate dispersions for [BMIM][NMsTFA] and their corresponding fittings using the model given by Eq. (7), recorded at 25°C **(a)** and 55°C **(b)**. Additionally, rotational contribution (Rot), homonuclear (Diff_FF), and heteronuclear (Diff_HF) translational contributions are shown. Magenta dashed lines represent the fitting error. Frequencies are ^{19}F Larmor frequencies.

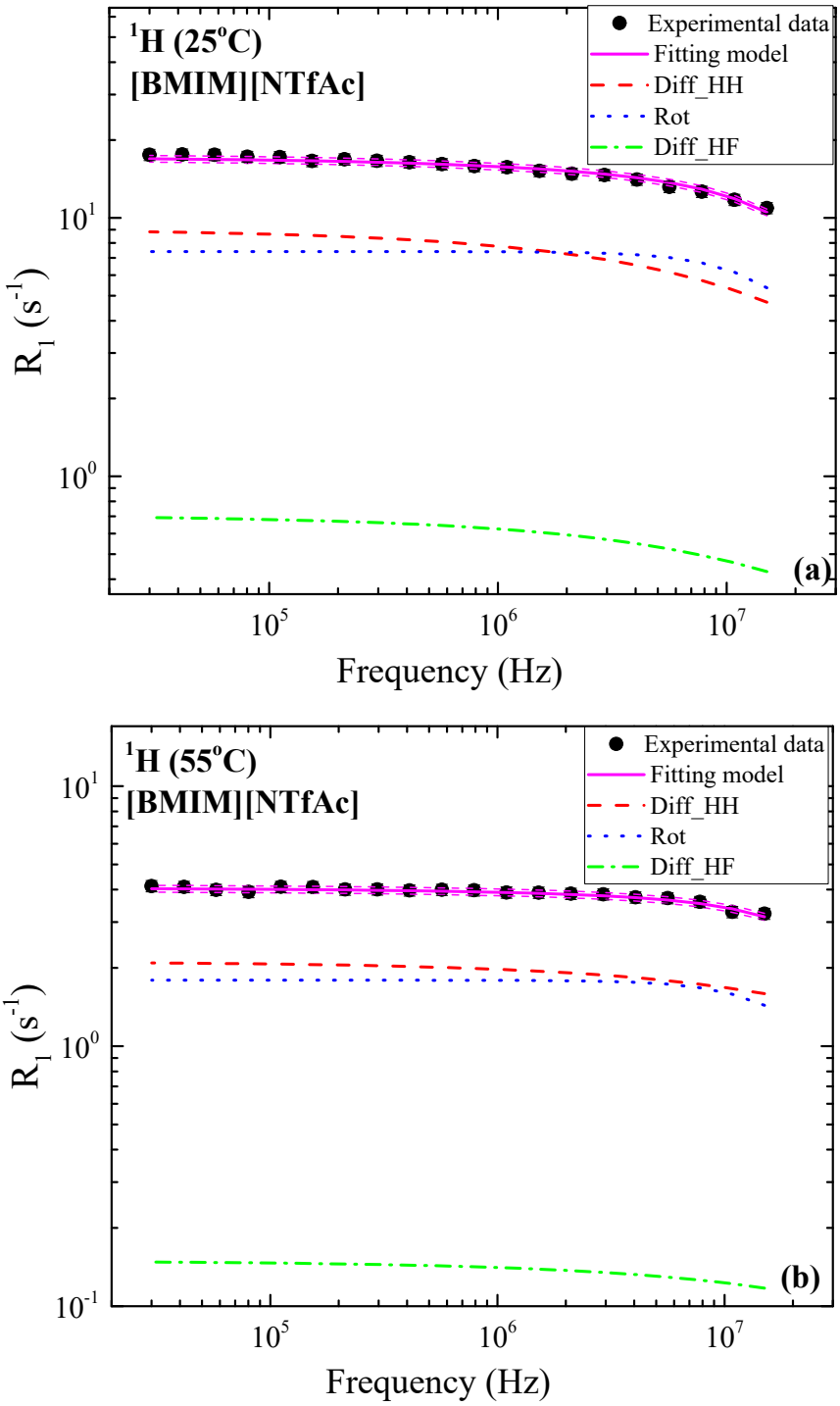

Figure S6. ^{1}H relaxation rate dispersions for [BMIM][NTfAc] and their corresponding fittings using the model given by Eq. (7), recorded at 25°C **(a)** and 55°C **(b)**. Additionally, rotational contribution (Rot), homonuclear (Diff_HH), and heteronuclear (Diff_HF) translational contributions are shown. Magenta dashed lines represent the fitting error. Frequencies are ^{1}H Larmor frequencies.

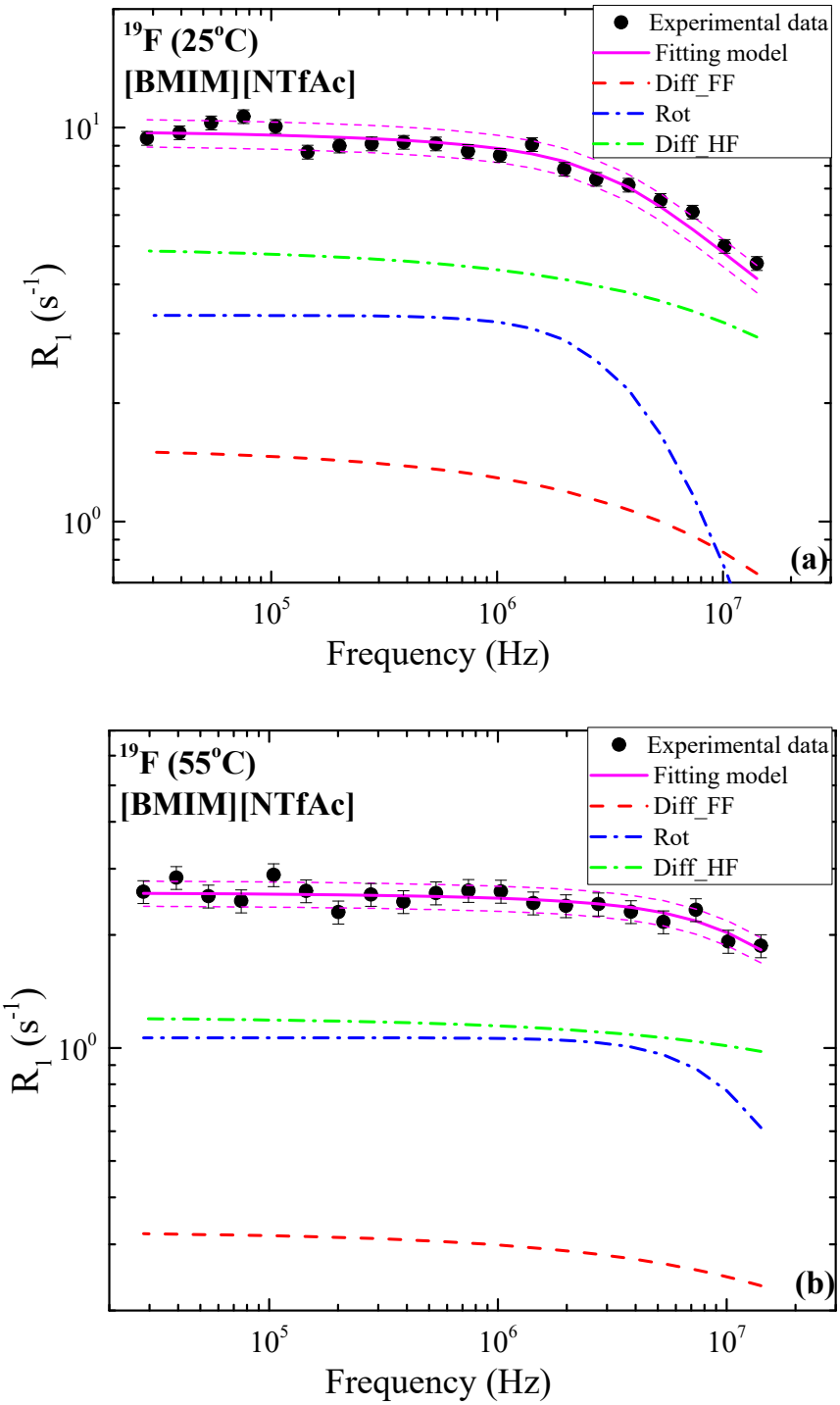

Figure S7. ^{19}F relaxation rate dispersions for [BMIM][NTfAc] and their corresponding fittings using the model given by Eq. (7), recorded at 25°C **(a)** and 55°C **(b)**. Additionally, rotational contribution (Rot), homonuclear (Diff_HH), and heteronuclear (Diff_HF) translational contributions are shown. Magenta dashed lines represent the fitting error. Frequencies are ^{19}F Larmor frequencies.

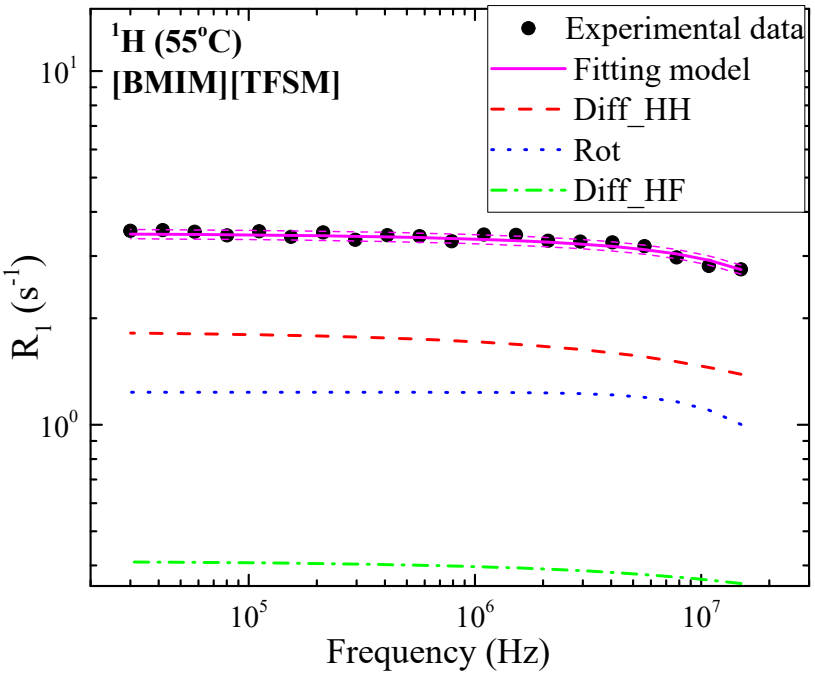

Figure S8. ^{1}H relaxation rate dispersion for [BMIM][TFSM] and its corresponding fitting using the model given by Eq. (7), recorded at 55°C. Additionally, rotational contribution (Rot), homonuclear (Diff_HH), and heteronuclear (Diff_HF) translational contributions are shown. Magenta dashed lines represent the fitting error. Frequencies are ^{1}H Larmor frequencies.

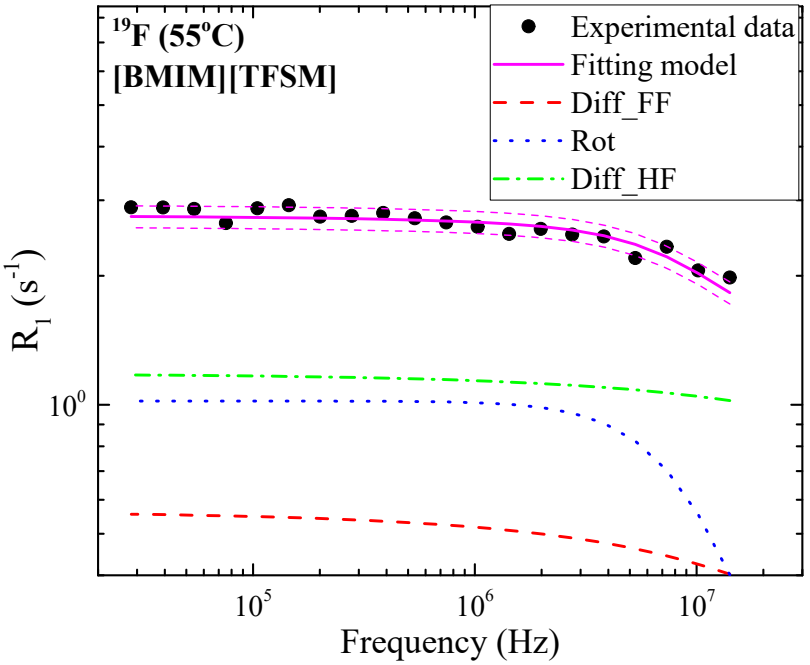

Figure S9. ^{19}F relaxation rate dispersion for [BMIM][TFSM] and its corresponding fitting using the model given by Eq. (7), recorded 55°C. Additionally, rotational contribution (Rot),

homonuclear (Diff_HH), and heteronuclear (Diff_HF) translational contributions are shown. Magenta dashed lines represent the fitting error. Frequencies are ^{19}F Larmor frequencies.

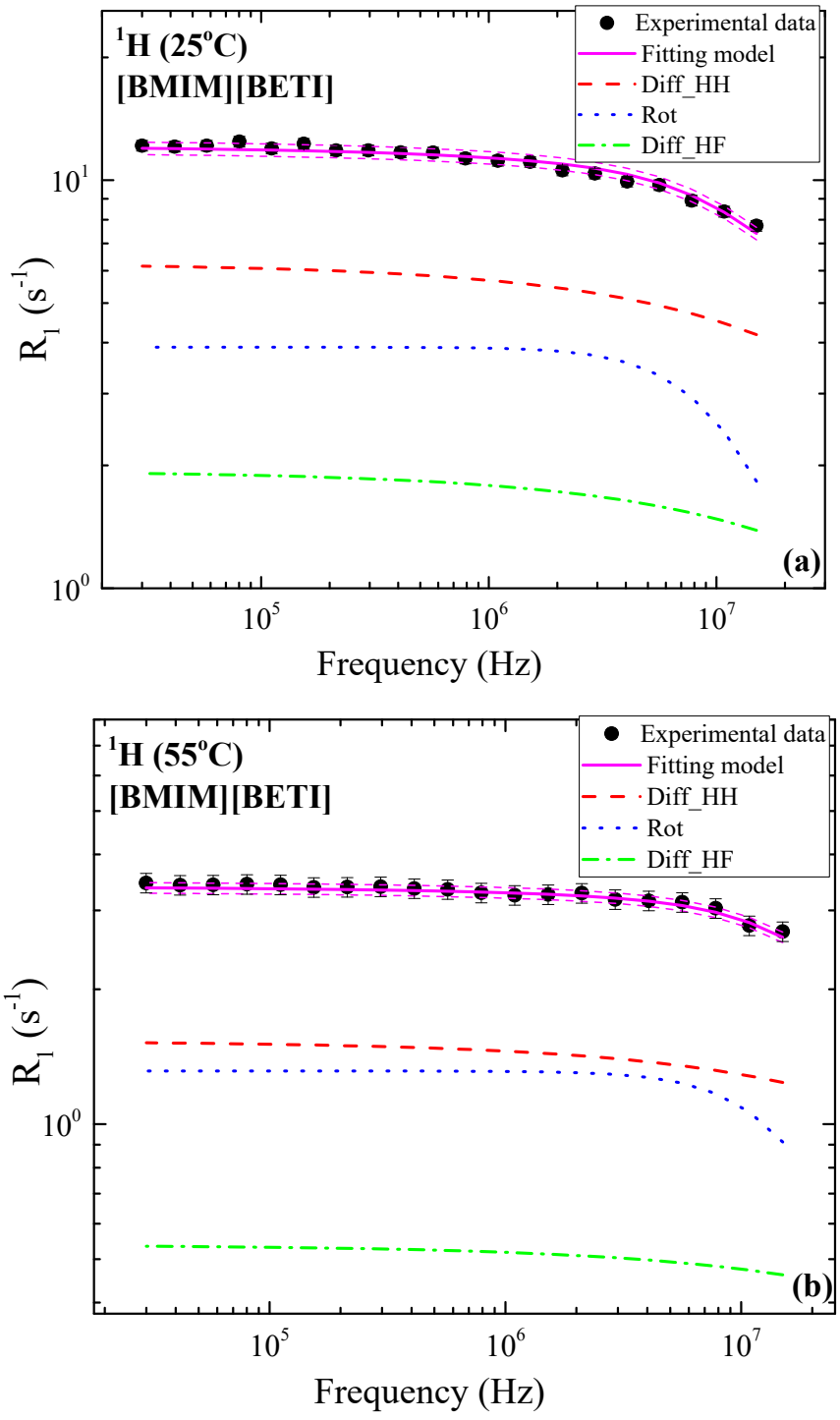

Figure S10. ^{1}H relaxation rate dispersions for [BMIM][BETI] and their corresponding fittings using the model given by Eq. (7), recorded at 25°C **(a)** and 55°C **(b)**. Additionally, rotational contribution (Rot), homonuclear (Diff_HH), and heteronuclear (Diff_HF) translational

contributions are shown. Magenta dashed lines represent the fitting error. Frequencies are ^{1}H Larmor frequencies.

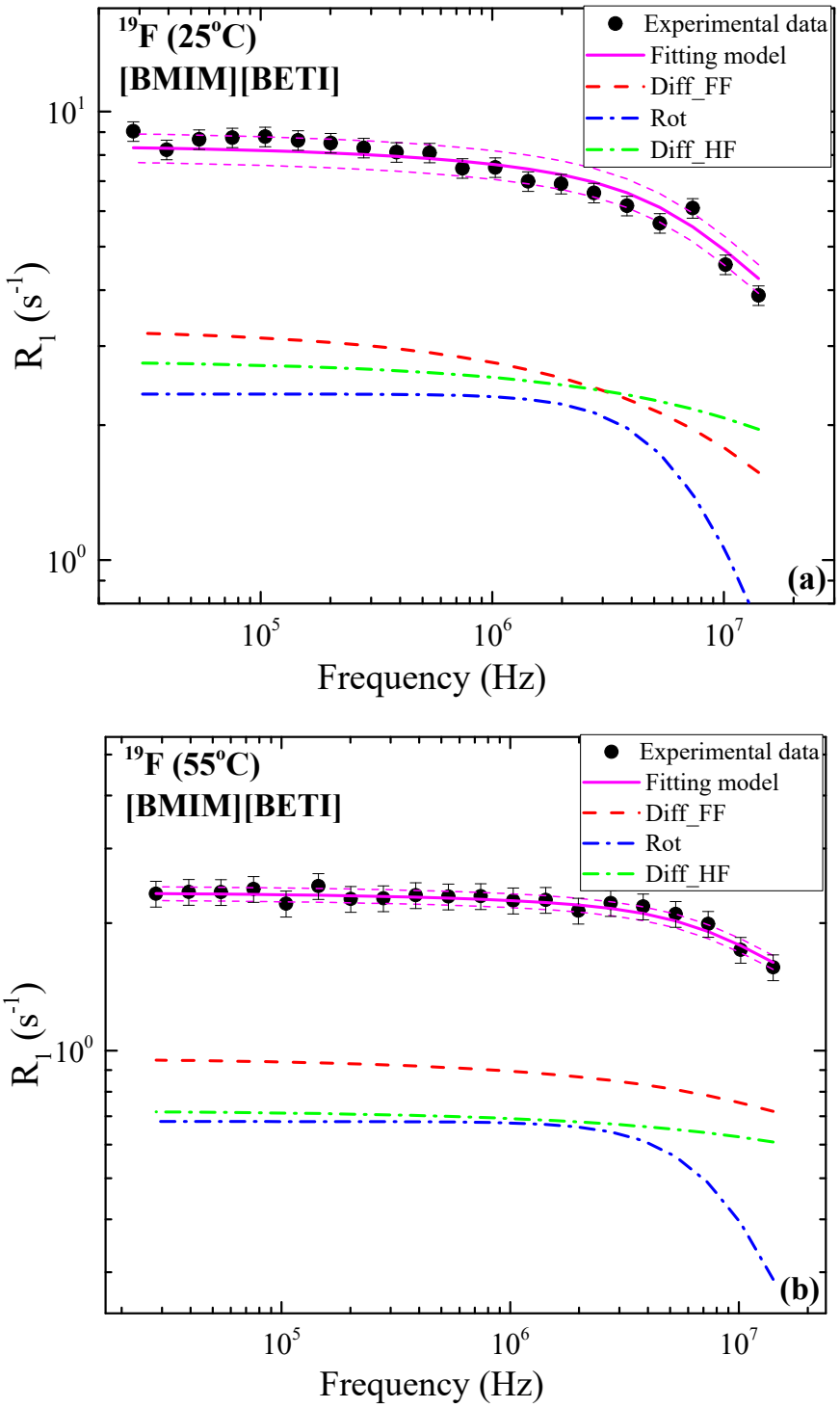

Figure S11. ^{19}F relaxation rate dispersions for [BMIM][BETI] and their corresponding fittings using the model given by Eq. (7), recorded at 25°C **(a)** and 55°C **(b)**. Additionally, rotational contribution (Rot), homonuclear (Diff_HH), and heteronuclear (Diff_HF)

translational contributions are shown. Magenta dashed lines represent the fitting error. Frequencies are ^{19}F Larmor frequencies.

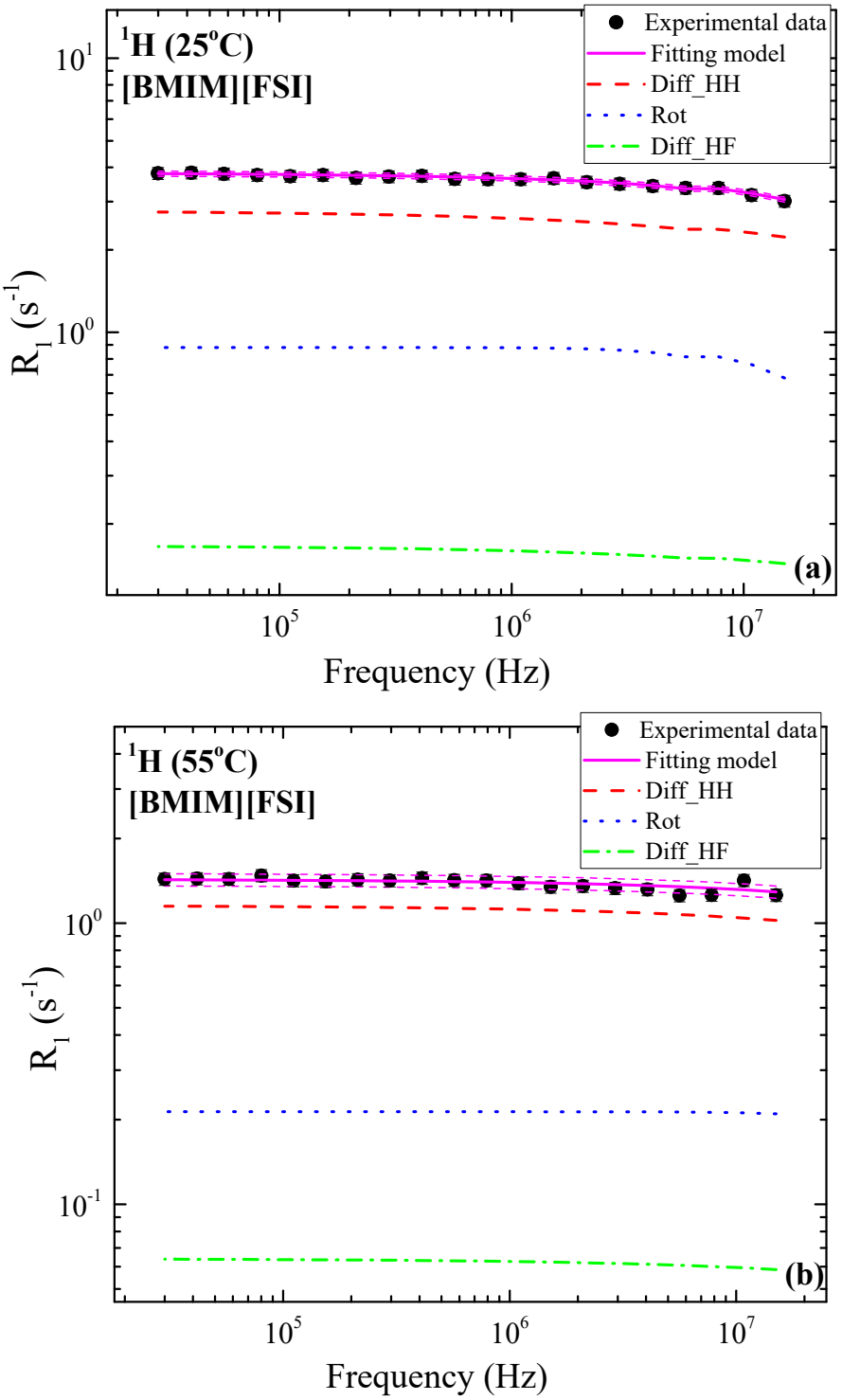

Figure S12. ^{1}H relaxation rate dispersions for [BMIM][FSI] and their corresponding fittings using the model given by Eq. (7), recorded at 25°C **(a)** and 55°C **(b)**. Additionally, rotational contribution (Rot), homonuclear (Diff_HH), and heteronuclear (Diff_HF) translational

contributions are shown. Magenta dashed lines represent the fitting error. Frequencies are ^{1}H Larmor frequencies.

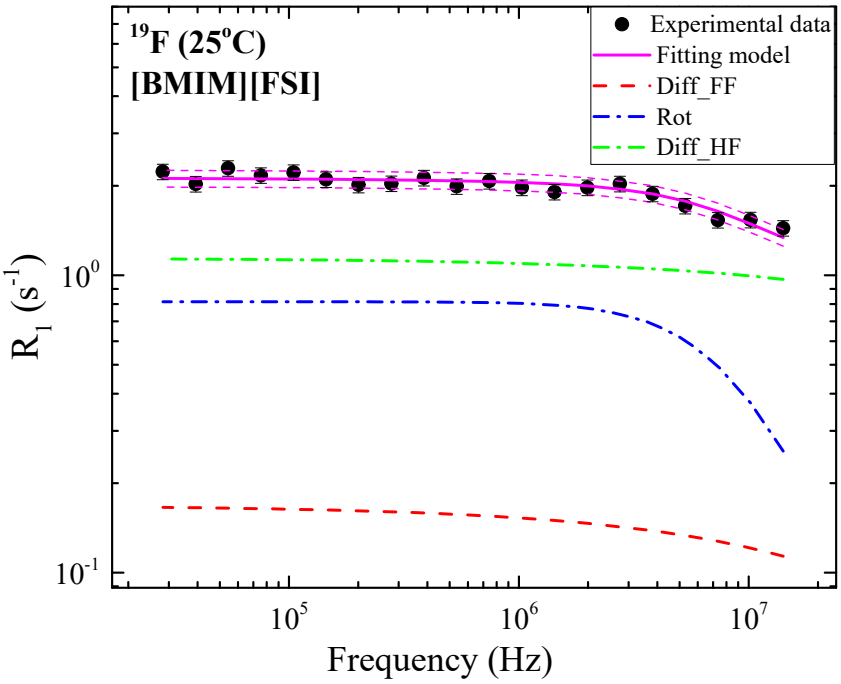

Figure S13. ^{19}F relaxation rate dispersions for [BMIM][FSI] and their corresponding fittings using the model given by Eq. (7), recorded at 25°C. Additionally, rotational contribution (Rot), homonuclear (Diff_HH), and heteronuclear (Diff_HF) translational contributions are shown. Due to the low signal-to-noise ratio, collecting anion dispersion data was impossible at 55°C. Magenta dashed lines represent the fitting error. Frequencies are ^{19}F Larmor frequencies.

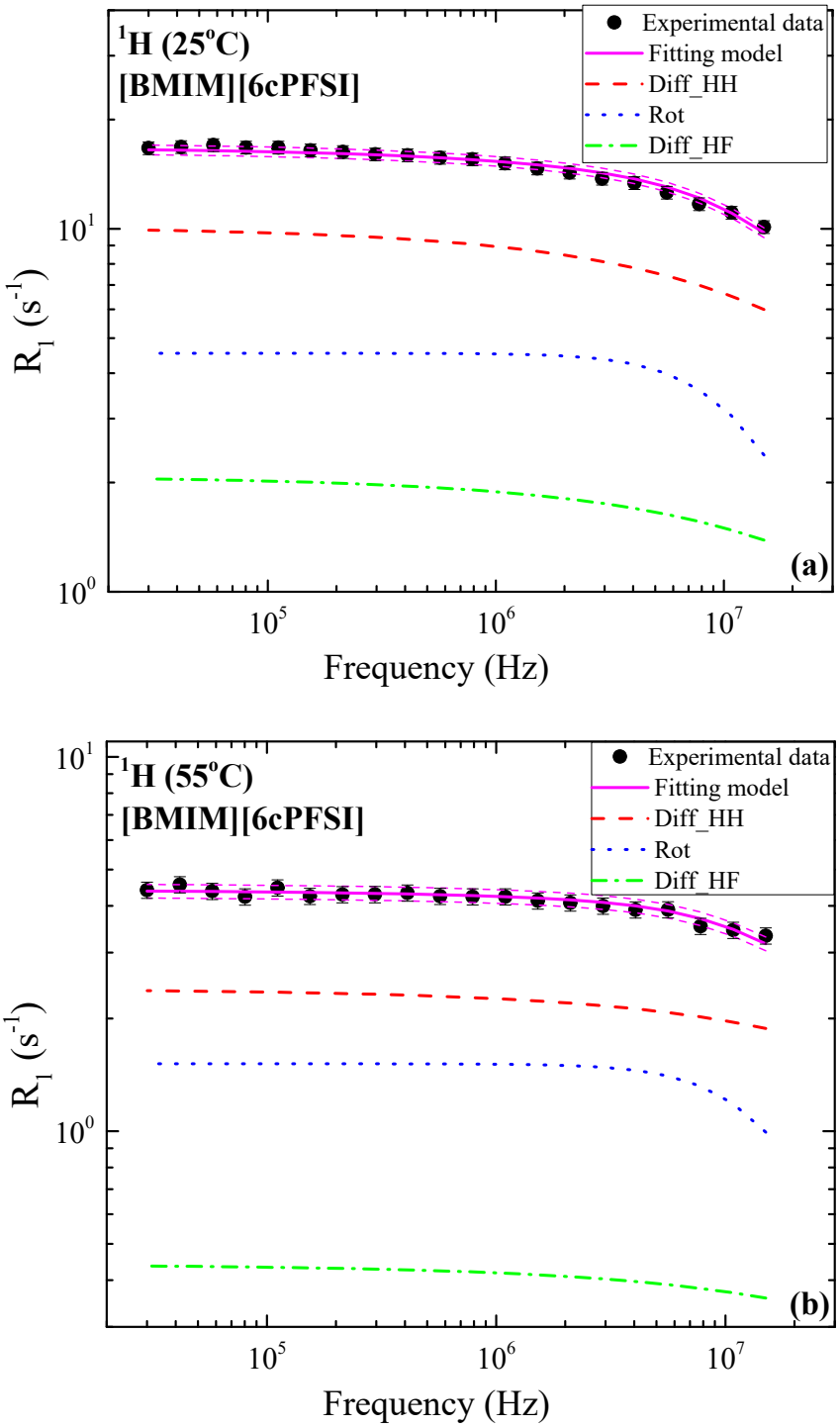

Figure S14. ^{1}H relaxation rate dispersions for [BMIM][6cPFSI] and their corresponding fittings using the model given by Eq. (7), recorded at 25°C **(a)** and 55°C **(b)**. Additionally, rotational contribution (Rot), homonuclear (Diff_HH), and heteronuclear (Diff_HF) translational contributions are shown. Magenta dashed lines represent the fitting error. Frequencies are ^{1}H Larmor frequencies.

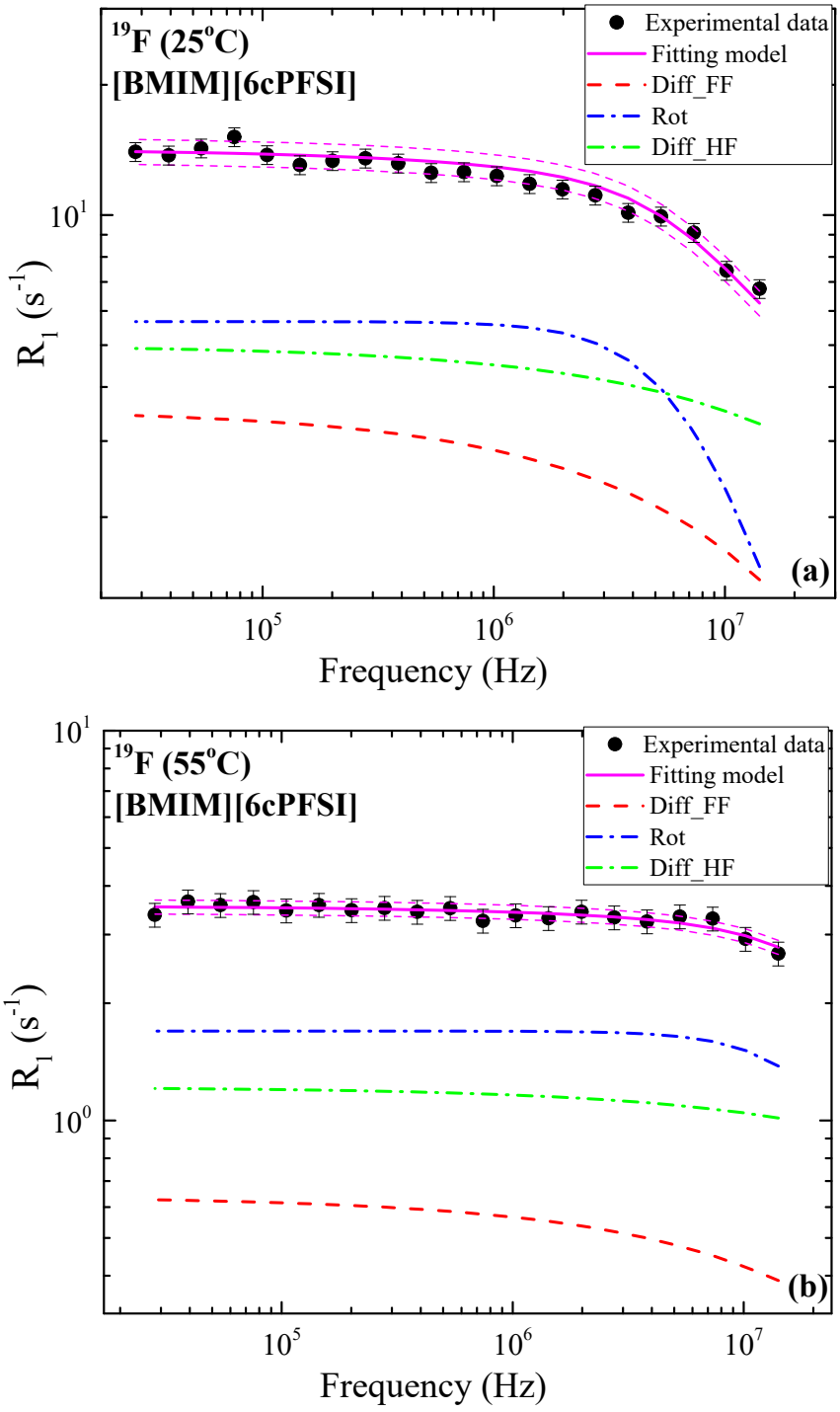

Figure S15. ^{19}F relaxation rate dispersions for [BMIM][6cPFSI] and their corresponding fittings using the model given by Eq. (7), recorded at 25°C **(a)** and 55°C **(b)**. Additionally, rotational contribution (Rot), homonuclear (Diff_HH), and heteronuclear (Diff_HF) translational contributions are shown. Magenta dashed lines represent the fitting error. Frequencies are ^{19}F Larmor frequencies.

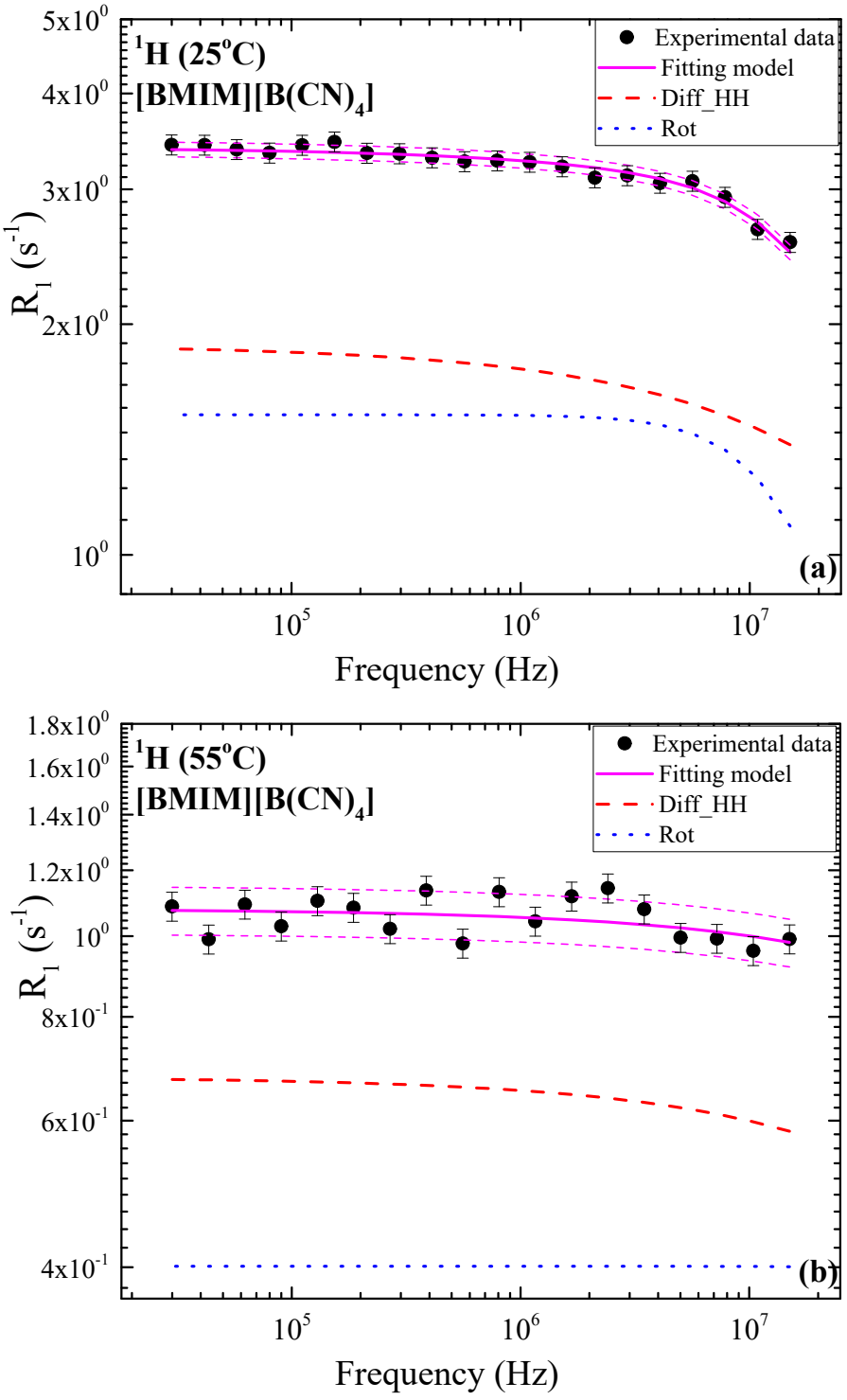

Figure S16. ^{1}H relaxation rate dispersions for [BMIM][B(CN)$_4$] and their corresponding fittings using the model given by Eq. (7), recorded at 25°C **(a)** and 55°C **(b)**. Rotational contribution (Rot), and homonuclear (Diff_HH) translational contribution are also shown. Magenta dashed lines represent the fitting error. Frequencies are ^{1}H Larmor frequencies.

3. Fitting parameters for the relaxation dispersions

Table S2. Parameters obtained using the model given by Eq. (7) to describe the longitudinal relaxation rate profiles for $[BMIM]^+$ (^1H) and the anions (^{19}F) of all studied ILs, at 25°C.

Parameters	[BMIM] [TFSM]		[BMIM] [NMsTFA]		[BMIM] [NTfAc]		[BMIM] [6cPFSI]		[BMIM] [BETI]		[BMIM] [FSI]		[BMIM] $[B(CN)_4]$
	^1H	^{19}F	^1H	^{19}F	^1H	^{19}F	^1H	^{19}F	^1H	^{19}F	^1H	^{19}F	^1H
d_{HH} [m] $\times10^{-10}$	3.4 ±0.2	-----	3.0 ±0.1	------	3.7 ±0.2	-----	2.8 ±0.1	------	2.7 ±0.1	------	2.7 ±0.1	------ -	3.6 ±0.1
d_{FF} [m] $\times10^{-10}$	-----	3.6 ±0.1	-----	3.1 ±0.2	-----	3.7 ±0.2	-----	3.8 ±0.2	------	3.9 ±0.2	------ -	4.7 ±0.2	-------
d_{HF} [m] $\times10^{-10}$	2.4 ±0.1	2.0 ±0.2	2.0 ±0.1	2.0 ±0.1	3.1 ±0.2	3.1 ±0.1	2.3 ±0.1	2.4 ±0.1	2.4 ±0.1	2.5 ±0.1	2.1 ±0.1	2.3 ±0.1	-------
D_H [m²/s] $\times10^{-12}$	9.9 ±0.1	9.7 ±0.3	5.0 ±0.1	4.9 ±0.2	10.1 ±0.3	7.7 ±0.8	8.8 ±0.1	8.8 ±0.2	12.8 ±0.2	12.7 ±0.2	41 ±2	40 ±1	42 ±1
D_F [m²/s] $\times10^{-12}$	7.9 ±0.3	8.0 ±0.2	4.1 ±0.1	4.1 ±0.1	7.6 ±0.3	7.7 ±0.2	5.7 ±0.2	5.7 ±0.1	8.8 ±0.2	8.5 ±0.3	40 ±1	40 ±3	-------
A_R [1/s²] $\times10^{8}$	2.0 ±0.1	0.5 ±0.1	3.8 ±0.2	0.3 ±0.1	4.1 ±0.1	0.40 ±0.05	1.6 ±0.1	1.0 ±0.1	1.20 ±0.08	0.50 ±0.03	0.60 ±0.04	0.20 ±0.04	0.80 ±0.05
τ_R [s] $\times10^{-9}$	5.1 ±0.2	17 ±1	5.9 ±0.3	59 ±3	3.6 ±0.2	17 ±1	5.7 ±0.3	10.9 ±0.7	6.4 ±0.3	10.0 ±0.5	3.2 ±0.1	9.8 ±0.5	3.7 ±0.2

Table S3. Parameters obtained using the model given by Eq. (7) to describe the longitudinal relaxation rate profiles for $[BMIM]^+$ (^1H) and the anions (^{19}F) of all studied ILs, at 55°C.

Parameters	[BMIM] [TFSM]		[BMIM] [NMsTFA]		[BMIM] [NTfAc]		[BMIM] [6cPFSI]		[BMIM] [BETI]		[BMIM] [FSI]	[BMIM] $[B(CN)_4]$
	^1H	^{19}F	^1H	^{19}F	^1H	^{19}F	^1H	^{19}F	^1H	^{19}F	^1H	^1H
d_{HH} [m] $\times10^{-10}$	3.4 ±0.1	------	3.2 ±0.1	------	3.5 ±0.1	------	2.8 ±0.1	------	2.8 ±0.1	------	2.5 ±0.1	3.3 ±0.1
d_{FF} [m] $\times10^{-10}$	-----	3.7 ±0.2	------	3.1 ±0.2	------	3.8 ±0.2	------	4.6 ±0.3	------	3.3 ±0.1	------	-------
d_{HF} [m] $\times10^{-10}$	2.1 ±0.1	2.0 ±0.1	2.1 ±0.1	2.0 ±0.1	3.3 ±0.2	2.7 ±0.2	2.5 ±0.1	2.6 ±0.1	2.2 ±0.1	2.4 ±0.1	2.1 ±0.1	-------
D_H [m²/s] $\times10^{-12}$	43 ±1	43 ±1	28 ±3	23 ±3	44 ±2	35 ±3	37 ±1	37 ±2	48 ±1	48 ±1	106 ±3	127 ±2
D_F [m²/s] $\times10^{-12}$	36 ±1	36 ±2	24 ±2	24 ±1	34 ±3	35 ±1	25 ±1	25 ±2	34 ±1	34 ±1	106 ±4	-------
A_R [1/s²] $\times10^{8}$	8.8 ±0.2	0.30 ±0.05	1.30 ±0.05	0.25 ±0.02	1.2 ±0.1	0.39 ±0.07	0.7 ±0.1	1 ±0.1	0.7 ±0.1	0.18 ±0.02	0.56 ±0.08	3.8 ±0.2
τ_R [s] $\times10^{-9}$	2.8 ±0.2	7.6 ±0.4	3.7 ±0.2	14 ±1	2.9 ±0.1	5.4 ±0.3	4.3 ±0.2	3.8 ±0.2	3.9 ±0.2	7.6 ±0.3	0.8 ±0.2	0.20 ±0.01